frontiers | Frontiers in Cellular and Infection Microbiology

TYPE Original Research
PUBLISHED 30 November 2022
DOI 10.3389/fcimb.2022.1021332

OPEN ACCESS

EDITED BY
Xing-Quan Zhu,
Shanxi Agricultural University, China

REVIEWED BY
Vyacheslav Yurchenko,
University of Ostrava, Czechia
Jack Sunter,
Oxford Brookes University,
United Kingdom

*CORRESPONDENCE
De-Hua Lai
laidehua@mail.sysu.edu.cn

†PRESENT ADDRESS
Yan-Zi Wen,
School of Pharmacology, Sun Yat-Sen University at East Campus,
Guangzhou, China

SPECIALTY SECTION
This article was submitted to Parasite and Host, a section of the journal Frontiers in Cellular and Infection Microbiology

RECEIVED 17 August 2022
ACCEPTED 03 November 2022
PUBLISHED 30 November 2022

CITATION
Wen Y-Z, Tang H-T, Cai X-L, Wu N, Xu J-Z, Su B-X, Hide G, Lun Z-R and Lai D-H (2022) *PAG3* promotes the differentiation of bloodstream forms in *Trypanosoma brucei* and reveals the evolutionary relationship among the *Trypanozoon* trypanosomes. *Front. Cell. Infect. Microbiol.* 12:1021332.
doi: 10.3389/fcimb.2022.1021332

PAG3 promotes the differentiation of bloodstream forms in *Trypanosoma brucei* and reveals the evolutionary relationship among the *Trypanozoon* trypanosomes

Yan-Zi Wen[1†], Hao-Tian Tang[1], Xiao-Li Cai[1], Na Wu[1], Jia-Zhen Xu[1], Bi-Xiu Su[1], Geoff Hide[2], Zhao-Rong Lun[1,2] and De-Hua Lai[1*]

[1]Guangdong Provincial Key Laboratory of Aquatic Economic Animals, Ministry of Education (MOE) Key Laboratory of Gene Function and Regulation, State Key Laboratory of Biocontrol, School of Life Sciences, Sun Yat-Sen University, Guangzhou, China, [2]Biomedical Research and Innovation Centre and Environment Research and Innovation Centre, School of Science, Engineering and Environment, University of Salford, Salford, United Kingdom

Introduction: Trypanosoma brucei, T. evansi and T. equiperdum are members of the subgenus Trypanozoon and are highly similar morphologically and genetically. The main differences between these three species are their differentiation patterns in the hosts and the role of vectors in their life cycles. However, the mechanisms causing these differences are still controversial.

Methods: PAG3 gene was accessed by PCR amplification in 26 strains of Trypanozoon and sequences were then analyzed by BLAST accompanied with T. evansitype B group. RNA interference and CRISPR/Cas9 were used for revealing possible role of PAG3 in slender to stumpy transformation.

Results: The procyclin associated gene 3 (PAG3) can be found in the pleomorphicspecies, T.brucei, which undergoes differentiation of slender forms to the stumpy form. This differentiation process is crucial for transmission to the tsetse fly vector. However, a homologue of PAG3 was not detected in either T. evansi or in the majority of T. equiperdum strains which are allmonomorphic. Furthere xperiments in T. brucei demonstrated that, when PAG3 was down-regulated or absent, there was a significant reduction in the differentiation from slender to stumpy forms.

Conclusion: Therefore, we conclude that PAG3 is a key nuclear gene involved in the slender to stumpy differentiation pathway of T.brucei in the

mammalian host. Loss of this gene might also offer a simple evolutionary mechanism explaining why T. evansi and some T. equiperdum have lost the ability to differentiate and have been driven to adapt to transmission cycles that by pass the tsetse vector or mechanical contact.

KEYWORDS

differentiation, procyclin associated gene, stumpy, *Trypanosoma brucei*, evolution, *Trypanozoon*

Introduction

Trypanosoma brucei is one of the members of the *Trypanozoon* group of trypanosomes and the pathogen that causes human sleeping sickness and the ruminant disease, Nagana, in Africa. To complete the life cycle, *T. brucei* needs to undergo differentiation stages to pass between the mammalian host and tsetse fly vector. Once invading the blood of the mammalian host, the metacyclic stage, derived from the vector, develops into the long slender form which is able to proliferate and escape host immunological attack by antigenic variation of the variant surface glycoprotein (VSG) coat (Cross, 1990). At a certain threshold density, the slender form trypanosomes differentiate into the cell cycle-arrested short stumpy form possessing a unique VSG. As they do not divide, stumpy cells will die in the mammalian bloodstream unless they differentiate into the procyclic forms in the midgut of the tsetse fly after a blood meal is taken. In the procyclic forms, the VSG coat of the trypanosome is shed and replaced by a stage-specific glycoprotein, the procyclin, which is considered to protect the trypanosomes from the digestive enzymes in the insect (Richardson et al., 1988; Roditi et al., 1998). In the subgenus *Trypanozoon*, alongside *T. brucei*, there are other two trypanosome species *T. equiperdum* and *T. evansi*, the causative agents of dourine and surra, respectively (Kostygov et al., 2021). They infect animals such as horses, camels and water buffaloes and account for a huge economic loss in many countries of Africa, South America and Asia. Unlike *T. brucei*, *T. evansi* and *T. equiperdum* cannot complete the cyclical development in the tsetse fly insect vector. *T. evansi* is mechanically transmitted by many bloodsucking insects, while *T. equiperdum* is transmitted during coitus.

Based on analyses, using a diverse range of biochemical and molecular characterizations, these three species have been shown to be genetically highly homologous to each other (Gibson et al., 1980; Lun et al., 1992a; Enyaru et al., 1993; Li et al., 2005; Wen et al., 2016). However, the obvious differences in the life cycle between these species suggest that there must be some genes controlling differentiation in *T. brucei* which should differ from those in *T. evansi* and *T. equiperdum*. In the last few decades, a wide range of studies have been carried out on the kinetoplast DNA (kDNA) of the members of the *Trypanozoon* subgenus and demonstrated that *T. equiperdum* and *T. evansi* have partially or totally lost elements of the kDNA in comparison with *T. brucei* (Borst et al., 1987; Ou et al., 1991; Lun et al., 1992b; Brun et al., 1998; Ventura et al., 2000; Lai et al., 2008). Therefore, it has been postulated that this loss of kDNA has locked the trypanosome in the bloodstream form stage, preventing survival in the tsetse, and has resulted in the evolution of alternative (mechanical) transmission among hosts. These studies further suggested that this was the reason why *T. evansi* and *T. equiperdum* have evolved from *T. brucei* and successfully spread out from Africa by developing an independence from the tsetse vector (Lun et al., 2010). Interestingly, however, some studies have contradicted this by indicating that *T. brucei* still retained the capacity of differentiation from the bloodstream form into procyclic form even when the kinetoplast DNA was artificially removed (Timms et al., 2002; Schnaufer et al., 2002). These results bring into doubt the notion that the kinetoplast and its genes are key factors that are essential for the differentiation of the bloodstream forms of *T. brucei* into the procyclic forms. Furthermore, some genes located in the trypanosome nucleus have been shown to be involved in the formation of the stumpy form (the precursor to the procyclic stage and the key stage in the mammalian bloodstream involved in infection of the vector). For example, it has been demonstrated that several trypanosomal proteins such as RBP7, YAK or MEKK1, TbGPR89 and others are involved in the stumpy induction factor signaling pathway and cell differentiation in *T. brucei* (McDonald et al., 2018; Silvester et al., 2018; Rojas et al., 2019). Furthermore, a recent study which generated monomorphic *T. brucei*, from a pleomorphic strain, confirmed that changes in the transcriptome of nuclear genes were associated with this transformation (Cai et al., 2022). Unlike kinetoplast DNA, which is required for the development and adaption in the insect, nuclear genes seem to perform a more important function in the differentiation between the mammalian bloodstream stages.

Recently, the genome of *T. evansi* (strain: STIB 805) has been sequenced and annotated (Carnes et al., 2014), as well as other trypanozoon species (Oldrieve et al., 2021). Interestingly, although the nuclear genome of *T. brucei* and *T. evansi* are extensively similar, the procyclic-associated gene 3 *(PAG3)* gene was

surprisingly discovered to be absent in this *T. evansi* strain. The *PAG* genes are located downstream within the same polycistronic transcription unit as the procyclin genes. They belong to a family of genes consisting of several different members and are named on the basis of their genomic loci and sequences (Vassella et al., 1994; Berberof et al., 1996; Liniger et al., 2001). To date, the function of *PAGs* have been unknown and were only considered to be coordinately expressed alongside procyclin and involved in adaption to life in the insect vector. However, as both the insect lifecycle stage and *PAG3* are lost in *T. evansi* STIB 805, this raises the interesting question as to whether or not the two observations are linked and also raises several other, more specific, questions. Is the *PAG3* gene missing in all strains of *T. evansi* and *T. equiperdum* isolated from different regions? Does it play a critical function during the differentiation of *T. brucei*? If so, in which stages of the lifecycle of *T. brucei* does it act? In this study, we aim to address these fascinating and important questions.

Materials and methods

Ethics statement

All animals were treated under the protocols approved by the National Institute for Communicable Disease Control and Prevention and the Laboratory Animal Use and Care Committee of Sun Yat-Sen University under the license 2010CB53000. Infections were carried out in adult male Swiss mice.

Trypanozoon DNA preparation

Trypanozoon strains used in this study are shown in Table 1. Trypanosomes were purified by the DEAE cellulose (DE-52) method from the blood of infected mice (Lanham & Godfrey, 1970). Genomic DNA was isolated by standard procedures following a protocol previously described (Wen et al., 2016).

Genomic DNA amplification

Oligonucleotide primers (Fw 5'-GTTTGACA CCGTGGAGTT-3'& Rv 5'-AACAGCCACAAACAACCC-3') were designed to amplify the coding regions of *PAG3*. PCR reactions were performed in a final volume of 25 µl containing 1 µl DNA, 1*PCR buffer (10 mM Tri-HCl pH 8.3, 50 mM KCl, 1.5 mM $MgCl_2$) 200 µM of each dNTP, 0.25 µM primer and 0.5 U Taq polymerase (Takara, China). The following cycling conditions were used, 98°C for 3 mins, followed by 35 cycles of 94°C for 30 sec, 55°C for 30 sec and 72°C for 2 min. PCR amplified fragments were analyzed on a 1% agarose gel, stained with ethidium bromide and photographed using a gel documentation system (UVITEC, Germany). The PCR amplifications and gel electrophoresis were repeated at least three times. PCR fragments were sent to be sequenced by Invitrogen (Thermo Fisher Scientific, China).

T. brucei cultivation and transformation

With the exception of the *PAG3* sequence comparisons, other experiments including RNA interference and gene knock-out were carried out using the *Trypanosoma brucei brucei* EATRO 1125 AnTat1.1 strain. *In vitro*, trypanosomes were cultured in HMI-9. Bloodstream forms of *T. brucei* were induced to differentiate into procyclic forms in SDM-79 containing 10% heat-inactivated fetal bovine serum (Gibco, Australia) by the additional 3 mM citrate and 3 mM cis-aconitate and incubated at 27°C with 5% CO_2 (Brun & Schonenberger, 1981).

Generation of cell lines

Bloodstream forms of *T. b. brucei* AnTat1.1, carrying integrated genes for T7 polymerase and the tetracycline repressor, were grown in HMI-9 medium. *PAG3* coding regions of 438 bp were amplified using the primers RNAi-Fw (5'-GGATCC GGAGTTAGAGGGCAAATGC-3') and RNAi-Rv (5'-AAGCTTTGGAAGTGCACTGAGTTACC-3') (Bam*HI* and Hind*III* restriction sites were included in the primers and are underlined) from the genome and inserted between the two opposing tetracycline inducible T7 RNA polymerase promoters of the plasmid vector p2T7-177. The construct was linearized with Not*I* and transfected into the bloodstream form of strain AnTat 1.1. Cells were cloned and selected with phleomycin as described (Wen et al., 2011).

To enable the use of CRISPR tools in *T. brucei* pleomorphic cells, we introduced the pJ1339 plasmid that carries a single resistance marker, puromycin, the tetracycline repressor, T7 RNA polymerase and Cas9, whose expression of Cas9 is constitutive, into *T. brucei* AnTat 1.1 cells. To knockout the endogenous copy of *PAG3*, the donor DNA for gene replacement contained pPOTv7 constructs (Blasticidin, Scarlet; Dean et al., 2015). *T. brucei* Cas9 T7 cells ($4x10^7$) were transfected with the PCR reactions containing 3 µg of two sgRNAs and 3 µg donor DNA in a total volume of 100 µl Human T Cell buffer from the Nucleofector™ Kit, using one pulse with program X-001 in the Amaxa Nucleofector IIb (Lonza, German). The correct construction of the clone was verified by PCR using the following primers P1 (5'-ATACCGAGGCTTCCACTAAG-3'), P2(5'-ATCCAAG CAAGCACATACAC-3'), P3(5'-GTTTGACACCGTGG AGTTG-3'), P4(5'-AACAGCCACAAACAACCC-3'), P5(5'-GCAACGGCTACAATCAAC-3') and P6 (5'-TATACGCTCCAGGCATCT-3') (Figure 1) (Beneke et al., 2017).

TABLE 1 Strains of *Trypanozoon* investigated in this study.

Strains	Species	Host/Vector	Origin	Isolation Date
TREU 927	*T. brucei*	Tsetse fly	Kenya	1970
AnTat1.1	*T. brucei*	Antelope	Uganda	1966
STIB 920	*T. brucei*	Hartebeest	Tanzania	1971
STIB 247-H	*T. brucei*	Hartebeest	Tanzania	1971
GVR 35	*T. brucei*	Hartebeest	Tanzania	1966
EATRO HN	*T. brucei*	n.a	n.a	n.a
STIB 164	*T. brucei*	n.a	n.a	n.a
STIB 777	*T. brucei*	Tsetse fly	Uganda	1971
Rho8	*T. brucei*	n.a.	n.a.	n.a.
Gzmb	*T. brucei*	n.a.	n.a.	n.a.
STIB 842	*T. equiperdum*	n.a.	n.a.	n.a.
STIB 841	*T. equiperdum*	n.a.	South Africa	n.a.
STIB 818	*T. equiperdum*	Horse	China	1979
STIB 784	*T. equiperdum*	n.a.	n.a.	n.a.
ATCC30019	*T. equiperdum*	n.a.	France	1903
CPO GZ	*T. evansi*	Water buffalo	China	2005
STIB 804	*T. evansi*	Water buffalo	China	1981
STIB 805	*T. evansi*	Water buffalo	China	1985
STIB 806	*T. evansi*	Water buffalo	China	1983
STIB 807	*T. evansi*	Water buffalo	China	1979
STIB 808	*T. evansi*	Water buffalo	China	1985
STIB 810	*T. evansi*	Water buffalo	China	1985
STIB 811	*T. evansi*	Water buffalo	China	1982
STIB 812	*T. evansi*	Water buffalo	China	1987
STIB 815	*T. evansi*	Horse	China	1964
STIB 816	*T. evansi*	Camel	China	1978
STIB 817	*T. evansi*	Mule	China	1964
STIB 821	*T. evansi*	n.a.	n.a.	n.a.
STIB 780	*T. evansi*	Camel	Kenya	1982
RoTat 1.2	*T. evansi*	Water buffalo	Indonesia	1982
AS 131M	*T. evansi*	Horse	Philippines	2006
SS 143M	*T. evansi*	Water buffalo	Philippines	2006
Stock Kazakh	*T. evansi*	Camel	Kazakhstan	1995
Stock Viet	*T. evansi*	Water buffalo	Vietnam	1998
Guangxi	*T. evansi*	Water buffalo	China	n.a.
Hubei	*T. evansi*	Water buffalo	China	n.a.

n.a., information not available.

Reverse transcription and quantitative real-time PCR

Aliquots of 20 μg of total RNA extracted from slender, stumpy and procyclic forms individually were treated with DNase I (Takara, China). cDNAs were synthesized using the PrimeScript RT reagent kits (Takara, China) following the standard protocol. A parallel reverse transcription reaction was also performed with the same amount of RNA without reverse transcriptase as a control for effective DNA contamination. Then cDNAs were diluted to the correct levels and prepared for quantitative PCR (qPCR). The housekeeping *β-tubulin* and AN1 genes were used as an external control (Kabani et al., 2009; Jones et al., 2014). The qPCR reactions were performed using the primers for *PAG3* (q-PAG3-Fw 5'-TTTCGTGCGGCGTGATTC-3' and q-PAG3-Rv 5'-TTCCCAAGGGCGGCAAGAG-3'), *PAD1*(q-PAD1-Fw 5'-ATCTGGAGCAATGCAAGCG-3' and q-PAD1-Rv 5'-AGATGAAGCTGTAGGGCAGC-3'), AN1 (AN1-F738 5'-GCGAGGAAACGGACCAAA-3' and AN1-R941 5'-CACATACACCAACAGCCACT-3') and *β-tu*bulin (q-tubulin-Fw 5'-CTGGCTTCAAGTGCGGTATCAA-3' and q-tubulin Rv 5'-GTACTCCTCCACATCCTCCTCG-3') with FastStart Universal SYBR Green Master on the Roche Light Cycler 480

Real-time Fluorescent Quantitative PCR System (Roche, Switzerland). The data were analyzed using the LightCycler480 Software1.5.

Analysis of cell differentiation

Identical quantities of wild type cells (2×10^5/mouse), RNAi constructed clone cells or deletion mutant cells were injected into the mice respectively. Specifically, a doxycycline drink (1 mg/ml + 50 mg/ml sucrose) was provided to the group of mice which were injected with RNAi clones to induce the inhibition, while the control group was provided with sucrose solution only. Tail blood smears were checked every day post infection in the RNAi and the control groups. The proportion of differentiating cells was analyzed on the basis of cell morphology (cell shape, the position of nuclei and kinetoplasts and the length of flagellum) of trypanosomes in blood smears stained with Giemsa (Dean et al., 2009). If trypanosomes differentiate to the stumpy form, which are identified as arresting in the 1K1N (one kinetoplast and one nuclei) configuration, the cell smears have a decreasing proportion of dividing cells (2K1N and 2K2N) (McDonald et al., 2018). Thus, the number of 1K1N cells were counted in the Giemsa stained blood smear collected at the peak (about 7×10^8/ml, 5 days post infection) in the deletion mutant group.

Statistical analysis

Statistical analysis was performed with Prism® 6.0 software (GraphPad Software Inc), using an unpaired Student's *t* test with Welch's correction (no assumption of equal standard deviation). P-values of less than 0.05 were considered significant. Data are presented as the mean ± standard deviation (SD).

Results

Investigation into the presence of the *PAG3* gene in *Trypanozoon* species

PAG3 has been reported to be found in the genomic unit EP3-PAG-GRESAG2.1 which is located on chromosome VI of *T. brucei* (Haenni et al., 2006). However, the function of *PAG3* in *T. brucei* is not clear. Due to the complete absence of this gene in the sequence of the strain (STIB 805) of *T. evansi* (Carnes et al., 2014), we proposed that it might play some biological function in the distinction between these trypanosomes. In order to analyze the presence/absence of *PAG3* in other strains of *T. evansi*, as well as strains of *T. equiperdum* and *T. brucei*, we designed PCR primers upstream (-517 bp) of the initiation codon and downstream (+179 bp) of the stop codon to amplify the *PAG3* gene. PCR amplification was conducted on thirty-six strains of *Trypanozoon*, including ten *T. brucei* strains, five *T. equiperdum* strains and twenty-one *T. evansi* stains (Table 1). Interestingly, 1305 base pair sized PCR fragments were detected in all *T. brucei* strains as well as two strains of *T. equiperdum* (STIB 842 and STIB 841) (Figure 1A). However, only fragments of 237 bp were amplified in all strains of *T. evansi* and the other three strains of *T. equiperdum* (STIB 818, STIB 784 and ATCC 30019). Meanwhile, the difference in sizes of the *PAG3* genes across the *Trypanozoon* strains was confirmed by the sequence alignment of the PCR products. According to the sequencing results (the data that support the findings of this study are available in Genbank, reference numbers MT176170-MT176178), all the *T. evansi* and some of the *T. equiperdum* strains had consistently lost the genomic fragment of 1069 bp (Figure 2B). Closer inspection of the lost fragment showed its structure as being flanked by 8-bp tandem repeats "TGTTTGTT". When considering the retained repeat to be the upstream one, the lost fragment spanned between -414 bp to +654 bp (relative to the initiation codon). This missing segment of the genome included the coding region of *PAG3* and a part of the 5' and 3' UTRs (Figure 2B). The very precise deletion of this segment of *PAG3* tends to suggest a common evolutionary origin and a possible interpretation is that the tested *T. evansi* and the *PAG3* deficient *T. equiperdum* strains are monophyletic. Interestingly, in a recent study (Oldrieve et al., 2021) reports the presence of another clade of *T. evansi* (type B) which also contains a recently identified *T. equiperdum* strain (IVM-t1). We did not have these strains to look at in our study but the genome of the latter strain has been recently sequenced and there is also available sequence data from the MU10 strain (a type B *T. evansi*). Interestingly, these both contain the *PAG3* gene, however, the sequences available show that there are possible indels and frameshifts in both strains (Figure 3A). Although these frameshifts would still need to be verified, it suggests another possible mechanism by which *PAG3* function could have been inactivated and that the loss of *PAG3* may have arisen more than once in *Trypanozoon*. However, the question still remains as to whether this gene is responsible for the loss of differentiation into tsetse-compatible life cycle stages.

PAG3 has elevated expression in the stumpy form of *T. brucei*

The lack of the life cycle stages in the vector, and the absence of the *PAG3* gene in some strains of *T. equiperdum* and all strains of *T. evansi*, raises some interesting questions. Is *PAG3* a key element involved in trypanosome differentiation and at which life cycle stage does it primarily act? As *PAG* genes have been found in the same transcription unit as the procyclin genes, they have been considered to be co-expressed with procyclin (Vassella et al., 1994). Procyclins are known to be the key surface

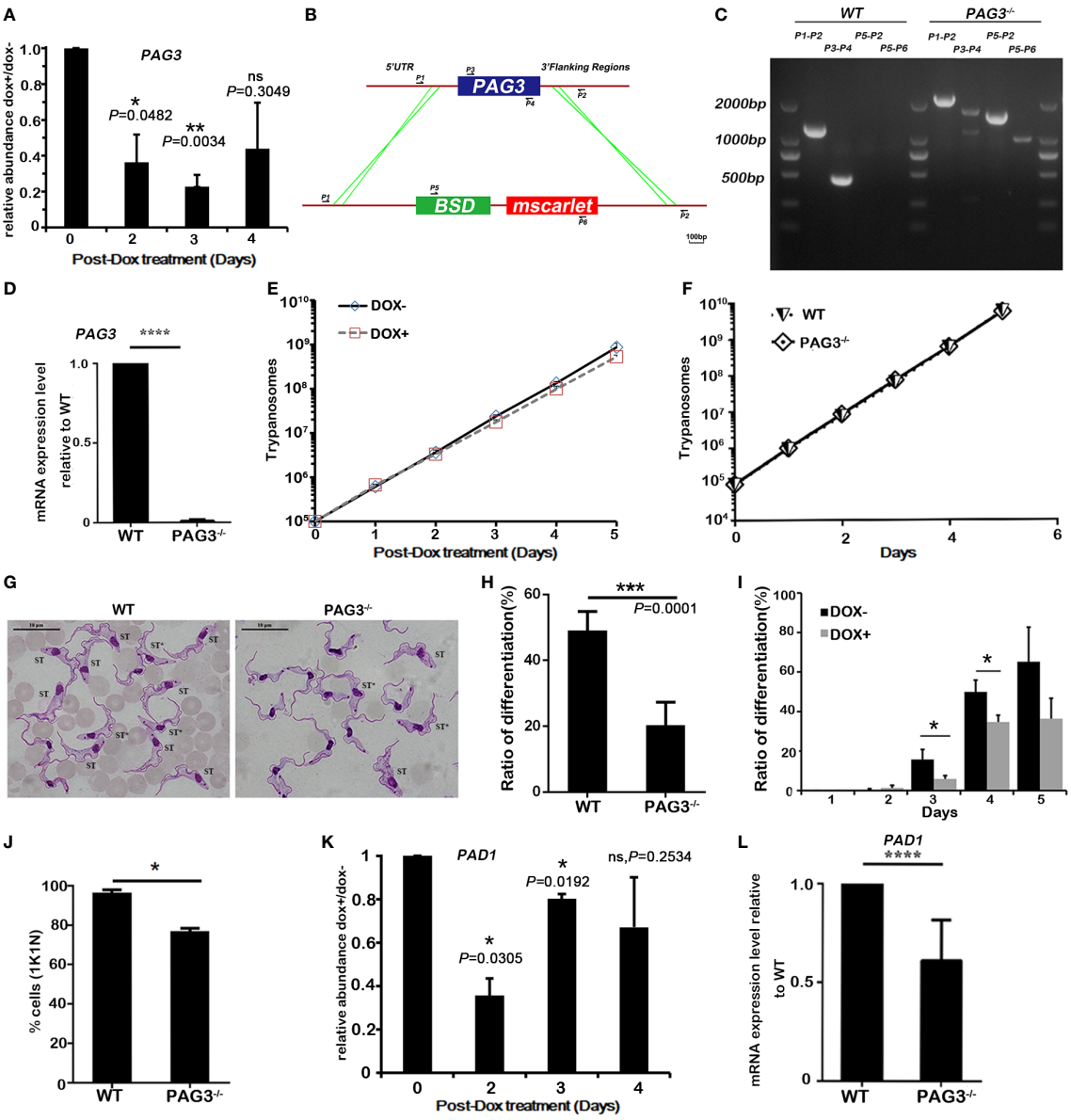

FIGURE 1
Expression of *PAG3* promotes stumpy form differentiation in *T. brucei*. **(A)** Quantitative real-time PCR analysis of RNA levels of *PAG3* in conditional knockdown cell lines. The relative abundance of the induced cells (DOX+) compared to the non-induced cells (DOX-) was plotted. These values were normalized using the transcripts of the housekeeping gene β-tubulin whose levels are not affected by RNAi. Error bars represent SD, n=3, 3 experiments. **(B, C)**. PCR-amplification system for verifying the CRISPR-Cas9 knockout clone. Primer pairs 1 and 2, 3 and 4, 3 and 2 were used to amplify the intact or partial *PAG3* coding gene. Primer pair 5 and 6 was used for identifying the drug selected gene BSD and fluorescent protein gene tagging. **(D)** The quantitative PCR analysis of RNA expression levels of *PAG3* in wild-type cell lines and *PAG3* deleted cell lines. These values have been normalized using the transcripts of AN1. Error bars represent SD (n=3), 3 experiments. **(E, F)** The growth curves of *T. brucei* wild-type cells (WT) *in vitro*, the *PAG3* conditional silenced clone **(E)** and the *PAG3* knock-out clone **(F)**. Cells were diluted to 1×10^5/ml and the number of cells were measured every 24 h. **(G)** The morphological analysis of trypanosomes isolated after 5 days post infection (the parasitemia was about 7×10^8/ml). Wild-type cells became morphologically stumpy with 1K1N (*Left*), while a higher proportion of *PAG3* knockout cells remained long and slender with 2K1N (*Right*). Nuclear and kinetoplast DNA was visualized by GIEMSA stain (Scale bar, 10 μm). ST* indicates intermediate form that transits from SL to ST. **(H)** The proportion of differentiated cells, including intermediate and stumpy forms, in G. **(I)** The proportion of differentiated cells, including intermediate and stumpy forms, in samples taken from day 2 to day 5 post infection for the *PAG3* RNAi induced cells (DOX+) or the non-induced cells (DOX-). Error bars represent SD (n=3 mice, about 200-300 trypanosomes for each group). **(J)** The proportion of 1K1N cells (a measure of growth arrested stumpy forms) in samples taken from day 5 post infection for the wild-type and the knock out cell lines. Error bars represent SD (n=3 mice, about 200 trypanosomes for each group). **(K, L)**. The quantitative real-time PCR analysis of RNA levels of *PAD1* in conditional *PAG3* knockdown cell lines (DOX+) compared with non-induced cells (DOX-) **(K)** and wild-type and *PAG3* knockout cell lines **(L)**. These values were normalized to the transcripts of the housekeeping gene β-tubulin **(K)** or AN1 **(L)**. Error bars represent SD, n=3, 3 experiments. Significance differences between to DOX+ and DOX- were indicated above the bars. Significances were accepted at *P<0.05, **P<0.01, ***P<0.001, ****P<0.0001, ns, not significant, using the Student's t test.

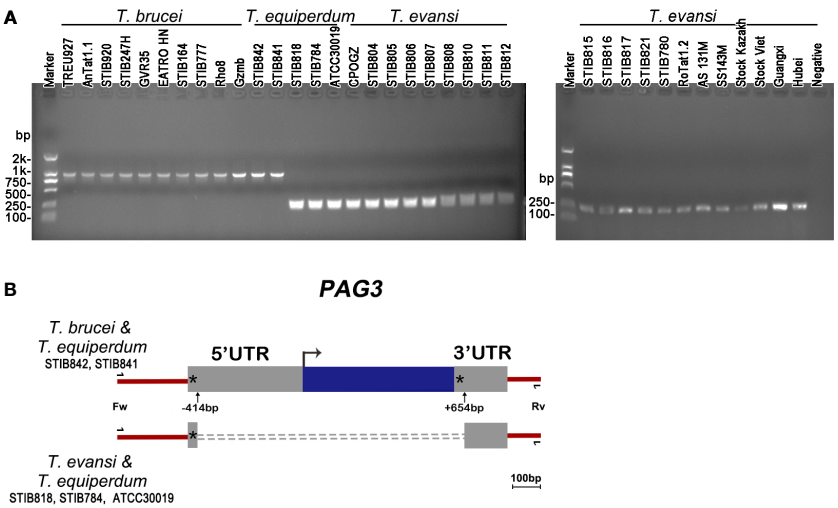

FIGURE 2
PAG3 genes in Trypanozoon species. **(A)** Electrophoretograms of PCR amplified fragments of the PAG3 genes in T. brucei, T. equiperdum and T. evansi. The information of the strains used in the PCR is listed in Table 1. **(B)** Schematic diagram showing a comparison of the PAG3 gene sequences across T. brucei, T. equiperdum and T. evansi. Blue box, the coding region; Grey boxes, the untranscribed regions; Asterisk, the 8-bp tandem repeat of TGTTTGTT; Dotted line, the absent fragment; Bent arrow, the initiation codon; Up arrow, the start and end positions of the absent fragment. The primers used for PCR is indicated.

antigens of *T. brucei* in the insect stage and are highly expressed in the procyclic form (Roditi et al., 1998). Therefore, it would follow that the *PAG* genes are most highly expressed in the procyclic stage. In order to test this hypothesis, we compared the expression of *PAG3* in different stages of *T. brucei* AnTat1.1 (slender, stumpy and procyclic forms) using real time PCR (Figure 3B, S1). Surprisingly, *PAG3* did not show the highest expression levels in the procyclic form of the insect vector, as expected, but it was significantly lower than that observed in the stumpy form (P=0.0257). Furthermore, expression levels were about 60% higher in the stumpy form than in the slender form of mammalian host (P<0.0001). This concurs with a similar result that was observed by high throughput RNA-Seq analysis (Naguleswaran et al., 2018).

PAG3 is involved in the differentiation of bloodstream forms in *T. brucei*

The differentiation of *T. brucei* in the mammalian host from the rapidly dividing slender form to the non-dividing stumpy form is a fascinating phenomenon in trypanosome biology (Dean et al., 2009; Kabani et al., 2009; Matthews, 2011; Jones et al., 2014; Saldivia et al., 2016; Zimmermann et al., 2017; Silvester et al., 2018; Matthews, 2021). Loss of this differentiation will induce malignancy in the trypanosomes and cause rapid death to the host in a similar manner to the uncontrolled spread of leukemia in multicellular organisms (Lun et al., 2015). However, although many studies have been carried out on the differentiation of *T. brucei*, the key mechanisms controlling differentiation in bloodstream forms are still unclear. Based on our results, we consider that the elevated expression of *PAG3* in stumpy forms suggests it has an important function in this stage or in the preadaptation to the insect midgut. In order to test this hypothesis, we performed *PAG3* RNA interference (Figure 1A) and CRISPR/Cas 9 knockout (Figures 1B–D) on the slender form of *T. brucei* (Antat1.1 strain) to silence or knock out the *PAG3* gene activity. *T. brucei* Antat1.1 is a good model system which displays pleomorphism (slender to stumpy conversion) in the blood of the infected mouse or rat. Our results indicated that *PAG3* is not essential for the survival of *T. brucei*, since the growth of the parasite cells did not significantly change after *PAG3* down-regulation or deletion *in vitro* (Figures 1E, F), and the parasitemia could reach 700 million per ml (Figure 1F, S2). As predicted by the hypothesis, the proportion of stumpy forms was significantly lower than the wild type cells with both the *PAG3* RNAi down regulation and in the knockout clones (Figures 1G–I). For instance, there was a reduction in the proportion of 1K1N cells, which represent cells not undergoing mitosis, which supports the reduction in the ratio of stumpy forms (Figure 1J). It is noteworthy that due to the reduced differentiation, the peak of the parasitemia in the *PAG3*$^{-/-}$ remains high and consequently led to the death of the mice (Figure S2), while the parental line differentiates and its parasitemia drops. Furthermore, we compared the expression of *PAD1*, a key marker of the stumpy form (Dean et al., 2009)

10.3389/fcimb.2022.1021332

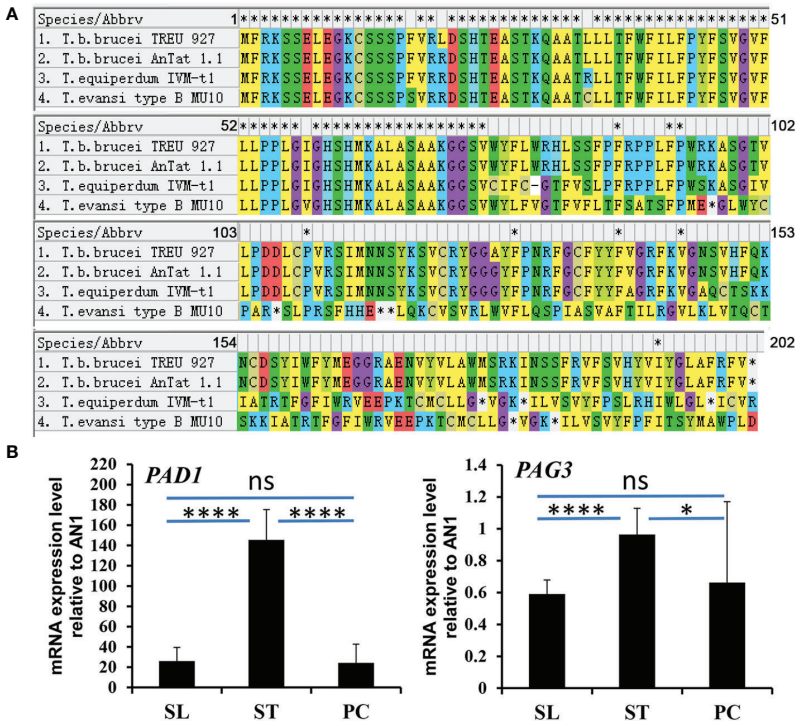

FIGURE 3
The alignment of PAG3 in T. brucei and its expression in different life stages of T. brucei. **(A)** The alignment of PAG3 in T. brucei with T. equiperdum IVM-t1 and T. evansi type B MU10. Possible frameshifts were found in T. equiperdum IVM-t1 and T. evansi type B MU10. **(B)** The expression of PAG3 in different life stages of T. brucei. The quantitative PCR analysis of RNA expression levels of PAD1 and PAG3 in different life stages of T. brucei. These values have been normalized to the transcripts of the Zinc finger protein (AN1). SL represents slender form; ST represents stumpy form; PF represents procyclic form. Error bars represent SD (n=3), 3 experiments. *P=0.0257, ****P<0.0001, ns, not significant (P=0.7461 in PAD1 and P=0.5576 in PAD1) using unpaired Student's t test with Welch's correction.

among the modified clones and wild type cells. In accordance with the morphological statistics, the expression of *PAD1* was significantly reduced in the conditional knock-down and knock-out cells (Figures 1K, L). Therefore, these results strongly demonstrate that the ability to differentiate from the slender form to the stumpy form was reduced when *PAG3* was deleted or down-regulated.

Discussion

In nature, *Trypanosoma evansi* and *T. equiperdum* only produce monomorphic slender forms in their mammalian hosts and are unable to develop in the insect vector or to be continuously cultivated *in vitro* at 27°C. The traditional view was that the incomplete component of kinetoplast DNA (kDNA) was an important factor in explaining why *T. equiperdum* and *T. evansi* fail to adapt in their insect vectors (Hoare, 1972; Brun et al., 1998; Lai et al., 2008). However, reports emerged that artificially produced dyskinetoplastic *T. brucei* cells (with incomplete kDNA) could develop into stumpy forms and progress further into procyclic forms, but lost the ability to divide (Timms et al., 2002). This showed that the full kinetoplast is important for further division and differentiation in the insect vector but may not be essential for transformation into the procyclic form. From our data, the complete lack of *PAG3* combined with the monomorphic phenotype found in all strains of *T. evansi*, that we looked at, and some strains of *T. equiperdum* suggest a strong link between the function of this gene and differentiation of the bloodstream forms of *Trypanozoon* parasites. A recent analysis of the relationships between *T. brucei*, *T. evansi* and *T. equiperdum*, using genome sequencing data, demonstrated the presence of two clades of *T. evansi* (Type A and B) (Cuypers et al., 2017; Oldrieve et al., 2021). A detailed look at a Type B strain (MU10) in the NCBI Sequence Read Archive, we found that the *PAG3* gene is probably present but appears to have indels and frameshifts which may possibly render it inactive. Interestingly, the annotation of a truncated *PAG3* gene in the Type A strain of *T. evansi*, STIB805, or TevSTIB805.6.480 in the TryTripDB database, was not detected by our PCR amplification experiments, indicating that this may be due to a possible artifact of assembly.

To our knowledge, there have been very few investigations into the function of *PAG3* in *T. brucei*. One important study concluded that *PAG3* was not essential for differentiation into the procyclic form as the deletion mutant was still able to establish a midgut infection (Haenni et al., 2006). However, they only focused on the transmission between distinct hosts and didn't investigate developmental changes in the mammalian bloodstream forms. In our study, we applied both RNAi and CRISPR/Cas9 methods to down-regulate and delete *PAG3* in *T. brucei*. Surprisingly, both the induced clones and mutants showed a significant reduction in differentiation from the slender form to the stumpy form in mice (Figure 1). These data provide evidence to suggest that *PAG3* has a role in *T. brucei* in promoting the formation of the stumpy form.

In mammalian blood, the trigger for differentiation from the slender to the stumpy form has been suggested to be dependent on the cell's capacity for quorum sensing (Zimmermann et al., 2017; Matthews, 2021), a process which requires secreted signals and receptor/transduction pathways to transmit the information between cells (Seed & Sechelski, 1989; Reuner et al., 1997). Several cell surface proteins have also been proved to be responsible for the transduction of stumpy induction factor (SIF) signaling within cells (Mony and Matthews, 2015; McDonald et al., 2018; Rojas et al., 2019). Interestingly, defects in quorum sensing pathways have recently been reported in *T. evansi* and *T. equiperdum* but also in artificially selected monomorphic lines of *T. brucei* (Cai et al., 2022). These parasites are normally almost indistinguishable from each other, using a wide range of molecular markers (Gibson et al., 1980; Lun et al., 1992a; Lun et al., 1992b; Lai et al., 2008; Verney et al., 2020), which makes it all the more interesting that these differences map onto the quorum sensing pathways. This implies a link between the acquisition of monomorphism and the loss of quorum sensing and supports the notion that *T. evansi* and *T. equiperdum* could have evolved from a malignant (or dedifferentiated) form of *T. brucei* (Lun et al., 2015). Interestingly, *PAGs* have been reported as potentially encoding membrane-associated or secreted proteins (Roditi et al., 1998; Liniger et al., 2001). The Tryptag data reveal *PAG3* is probably located in the cytoplasm and nuclear lumen of procyclic cells (Dean et al., 2017). Therefore, we suggest that *PAG3* might also be involved in stumpy formation by being a component of the SIF transduction system into the nucleus. To fully understand its function, more studies on the structure of *PAG3* and its interaction with other molecules in the pathway are certainly required.

Concerning the evolutionary relationship between *T. equiperdum* and *T. evansi*, *PAG3* may provide some clues. Interestingly, we found that the presence/absence of *PAG3* in *T. equiperdum* was divided into two groups. Although some strains of *T. equiperdum* have lost *PAG3* like *T. evansi*, others still possess the complete gene sequence like *T. brucei*. A key question is why these *T. equiperdum* strains still maintain this gene but yet are unable to differentiate. *T. equiperdum* has long been adapted for mechanical transmission and, although retaining the gene in some strains, the expression or function of *PAG3* might be lost. It is possible that the *PAG3*$^{+}$ strains of *T. equiperdum* have a mutation/defect in a different gene within the stumpy differentiation pathway which has rendered them monomorphic. This might support the notion that the genotypes of *T. equiperdum* have polyphyletic origins. This is supported by the studies of Oldrieve et al. (2021) who demonstrated, by genome analysis, that there is indeed more than one clade of *T. equiperdum* in the strains that they look at. Unfortunately, their strains do not correspond to our strains. Other studies have shown the existence or more than one genotype of *T. equiperdum* by RFLP (Zhang & Baltz, 1994), by RAPD and multiplex-endonuclease genotyping analysis (Claes et al., 2003; Lun et al., 2004). Furthermore, other studies have revealed that *T. equiperdum* strains were divided into two groups, related to either *T. brucei* or to *T. evansi* based on spliced leader RNA (slRNA) (Lai et al., 2008) and a heterogeneity (Class A & B) in the kinetoplast genome among *Trypanozoon* strains based on the composition of the maxicircles. Strains in Class A, including STIB 818, STIB 784 and ATCC 30019, lack some of the maxicircle genes which show similarity to the lack of maxicircles in *T. evansi* strains. Strains in Class B, including STIB 841 and STIB 842, contain a full maxicircle genome similar to that found in *T. brucei*. These results are exactly consistent with our findings for *PAG3* (Figure 2) with Class A and Class B being *PAG3*$^{-}$ and *PAG3*$^{+}$ strains respectively. Hence, evidence from both kinetoplast and nuclear gene analyses suggest that some strains of *T. equiperdum* still retain the same genomic characteristics as the ancestral *T. brucei* while the others have lost these genes during the evolution of long-term mechanical transmission. This view is supported by the latest reported isolate of *T. equiperdum* (IVM-t1) from Mongolia (Suganuma et al., 2016). This isolate has been found to be a lost link from *T. brucei* to a distinct type of *T. evansi* (Davaasuren et al., 2019; Oldrieve et al., 2021), and is characterized by possessing a possible frameshifted *PAG3* gene.

On the other hand, *PAG3* was found to be lost in all of the type A strains of *T. evansi* we examined. However, the type B strains reported recently (Oldrieve et al., 2021) may also have a possible frameshifted *PAG3* as found in IVM-t1. These may support the hypothesis that *T. evansi* is likely to have polyphyletic origins (Njiru et al., 2006). Both situations in *PAG3* (deleted or frameshifted) were found in both *T. equiperdum* and *T. evansi*, suggesting that each *T. equiperdum* strain could be the ancestral source of their corresponding *T. evansi* strains.

The occurrence of gene deletions in both the nuclear and kinetoplast genomes of *T. evansi* and *T. equiperdum* raises an interesting question as to which happened first in evolutionary terms? The proteins encoded in the kinetoplast are proposed to be responsible for adaption to the insect vector rather than

differentiation of bloodstream forms (Brun et al., 1998; Timms et al., 2002; Lai et al., 2008). In the present study, we have demonstrated that *PAG3* is involved in the formation of the stumpy form, a role probably shared with other nuclear genes such as RBP7, YAK or MEKK1 (Mony and Matthews, 2015). In the mammalian host, only the stumpy form of *T. brucei* is able to differentiate into procyclic form in the insect vector. Thus, we may speculate that in the ancestral *T. brucei*, the nuclear genes, such as *PAG3*, involved in differentiation from slender form to stumpy form might be lost first and thus driving the evolution of the parasite towards mechanical transmission. These variants then lost kinetoplast genes (including the RNA editing guide functions), which were no longer required, since they could be mechanically transmitted from host to host. Today, these mutated monomorphic trypanosomes are called *T. equiperdum* and *T. evansi* depending on their host specificity. Although a further complication is raised in that the study of Oldrieve et al. (2021) has demonstrated that the apparent *T. equiperdum* strains IVM-t1, isolated from horses, is actually located within the *T. evansi* type B clade. Thus host range may no longer be a clear distinguishing feature of these species.

Based on the presence or absence of the *PAG3* gene among *Trypanozoon* strains, we have another tool for distinguishing between clades within this group. Although further work may be needed to definitively identify which clades are $PAG3^{+}$ and $PAG3^{-}$, we can now more easily distinguish and diagnose these species in the laboratory, in the field or the clinic, and thereby improve health outcomes for infected patients or animals.

In conclusion, we have demonstrated significant differences in the *PAG3* gene among the species in the subgenus *Trypanozoon*. Furthermore, we have demonstrated that *PAG3* is involved in the transformation of *T. brucei* from the bloodstream slender form to the stumpy form. These results have not only discovered a novel molecule involved in the differentiation of the bloodstream form of *T. brucei* but also provided novel evidence which further clarifies the evolutionary status of *T. evansi* and *T. equiperdum*.

Data availability statement

The datasets presented in this study can be found in online repositories. The names of the repository/repositories and accession number(s) can be found in the article/Supplementary Material.

Ethics statement

The animal study was reviewed and approved by National Institute for Communicable Disease Control and Prevention and the Laboratory Animal Use and Care Committee of Sun Yat-Sen University.

Author contributions

Conceptualization: Y-ZW and Z-RL; methodology: Y-ZW and D-HL; formal analysis: Y-ZW, H-TT, and X-LC; Investigation: Y-ZW, X-LC, NW, J-ZX, and B-XS; visualization: Y-ZW, H-TT, X-LC, and D-HL; project administration: Z-RL and D-HL; funding acquisition: Z-RL and D-HL; writing – original draft: Y-ZW, D-HL, and Z-RL; writing – review and editing: H-TT, GH, D-HL, and Z-RL. All authors contributed to the article and approved the submitted version.

Funding

This work was supported by the grants from the National Natural Science Foundation of China (#31672276, #31720103918, #32270446) and the Natural Science Foundation of Guangdong Province (#2022A1515011874, #2018A030313187).

Acknowledgments

We thank Dr. Jack Sunter, Oxford Brookes University, UK who provided the 1339 plasmid, and Ms. Yu-Bei Liang's help in qPCR experiments.

Conflict of interest

The authors declare that the research was conducted in the absence of any commercial or financial relationships that could be construed as a potential conflict of interest.

Publisher's note

Supplementary material

The Supplementary Material for this article can be found online at: https://www.frontiersin.org/articles/10.3389/fcimb.2022.1021332/full#supplementary-material

References

Beneke, T., Madden, R., Makin, L., Valli, J., Sunter, J., and Gluenz, E. (2017). A CRISPR Cas9 high-throughput genome editing toolkit for kinetoplastids. *R. Soc. Open Sci.* 4, 170095. doi: 10.1098/rsos.170095

Berberof, M., Pays, A., Lips, S., Tebabi, P., and Pays, E. (1996). Characterization of a transcription terminator of the procyclin PARP a unit of *Trypanosoma brucei*. *Mol. Cell. Biol.* 55, 135–145. doi: 10.1128/MCB.16.3.914

Borst, P., Fase-Fowler, F., and Gibson, W. C. (1987). Kinetoplast DNA of *Trypanosoma evansi*. *Mol. Biochem. Parasitol.* 23, 31–38. doi: 10.1016/0166-6851(87)90184-8

Brun, R., Hecker, H., and Lun, Z. R. (1998). *Trypanosoma evansi* and *T. equiperdum*: distribution, biology, treatment and phylogenetic relationship (a review). *Veterinary Parasitol.* 79, 95–107. doi: 10.1016/S0304-4017(98)00146-0

Brun, R., and Schonenberger, M. (1981). Stimulating effect of citrate and cis-aconitate on the transformation of *Trypanosoma brucei* bloodstream forms to procyclic forms *in vitro*. *Z Parasitenkd* 66, 17–24. doi: 10.1007/BF00941941

Cai, X. L., Li, S. J., Zhang, P., Li, Z., Hide, G., Lai, D. H., et al. (2022). The occurrence of malignancy in *Trypanosoma brucei brucei* by rapid passage in mice. *Front. Microbiol.* 12, 806626. doi: 10.3389/fmicb.2021.806626

Carnes, J., Anupama, A., Balmer, O., Jackson, A., Lewis, M., Brown, R., et al. (2014). Genome and phylognenetic analyses of *Trypanosoma evansi* reveal extensive similarity to *T. brucei* and multiple independent origins for dyskinetoplasty. *PloS Negl. Trop. Dis.* 9, e3404. doi: 10.1371/journal.pntd.0003404

Claes, F., Agbo, E. C., Radwanska, M., Te Pas, M. F., Baltz, T., Dewaal, D. T., et al. (2003). How does *Trypanosoma equiperdum* fit into the *Trypanzoon* group? a cluster analysis by RAPD and multiplex-endonuclease genotyping approach. *Parasitology* 126, 425–431. doi: 10.1017/S0031182003002968

Cross, G. A. M. (1990). Cellular and genetic aspects of antigenic variation in trypanosomes. *Annu. Rev. Immunol.* 8, 83–110. doi: 10.1146/annurev.iy.08.040190.000503

Cuypers, B., Van den Broeck, F., Van Reet, N., Meehan, C. J., Cauchard, J., Wilkes, J. M., et al. (2017). Genome-wide SNP analysis reveals distinct origins of *Trypanosoma evansi* and *Trypanosoma equiperdum*. *Genome Biol. Evol.* 9, 1990–1997. doi: 10.1093/gbe/evx102

Davaasuren, B, Yamagishi, J, Mizushima, D, Narantsatsral, S, Otgonsuren, D, Myagmarsuren, P, et al (2019). Draft genome sequence of *Trypanosoma equiperdum* strain IVM-t1. *Microbiol Resour Announc* 8, e01119-18. doi: 10.1128/MRA.01119-18

Dean, S., Marchetti, R., Kirk, K., and Matthews, K. R. (2009). A surface transporter family conveys the trypanosome differentiation signal. *Nature* 459, 213–217. doi: 10.1038/nature07997

Dean, S., Sunter, J., and Wheeler, R. J. (2017). TrypTag.org: a trypanosome genome-wide protein localisation resource. *Trends Parasitol.* 33, 80–82. doi: 10.1016/j.pt.2016.10.009

Dean, S., Sunter, J., Wheeler, R. J., Hodkinson, I., Gluenz, E., and Gull, K. (2015). A toolkit enabling efficient, scalable and reproducible gene tagging in trypanosomatids. *Open Biol.* 5, 140197. doi: 10.1098/rsob.140197

Enyaru, J. C., Stevens, J. R., Odiit, M., Okuna, N. M., and Carasco, J. F. (1993). Isoenzyme comparison of trypanozoon isolates from two sleeping sickness areas of south-eastern Uganda. *Acta Tropica* 55, 97–115. doi: 10.1016/0001-706X(93)90072-J

Gibson, W. C., Marshall, T. F., and Godfrey, D. G. (1980). Numerical analysis of enzyme polymorphism: a new approach to the epidemiology and taxonomy of trypanosomes of the subgenus trypanozoon. *Adv. Parasitol.* 18, 175–246. doi: 10.1016/S0065-308X(08)60400-5

Haenni, S., Renggli, K. C., Fragoso, M. C., Oberle, M., and Roditi, I. (2006). The procyclin-associated genes of trypanosoma brucei are not essential for cyclical transmission by tsetse. *Mol. Biochem. Parasitol.* 150, 144–156. doi: 10.1016/j.molbiopara.2006.07.005

Hoare, C. A. (1972). *The trypanosomes of mammals. a zoological monograph* (Oxford: Blackwell), 555–592.

Jones, N. G., Thomas, E. B., Brown, E., Dickens, N. J., Hammarton, T. C., and Mottram, J. C. (2014). Regulators of trypanosoma brucei cell cycle progression and differentiation identified using a kinome-wide RNAi screen. *PLoS Pathog.* 10, e1003886. doi: 10.1371/journal.ppat.1003886

Kabani, S., Fenn, K., Ross, A., Ivens, A., Smith, T. K., Ghazal, P., et al. (2009). Genome-wide expression profiling of in vivo-derived bloodstream parasite stages and dynamic analysis of mRNA alterations during synchronous differentiation in trypanosoma brucei. *BMC Genomics* 10, 427. doi: 10.1186/1471-2164-10-427

Kostygov, A. Y., Karnkowska, A., Votýpka, J., Tashyreva, D., Maciszewski, K., Yurchenko, V., et al. (2021). Euglenozoa:taxonomy, diversity and ecology, symbioses and viruses. *Open Biol.* 11, 200407. doi: 10.1098/rsob.200407

Lai, D. H., Hashimia, H., Lun, Z. R., Ayala, J. F., and Lukes, F. (2008). Adaptations of trypanosoma brucei to gradual loss of kinetoplast DNA: Trypanosoma equiperdum and trypanosoma evansi are petite mutants of t. brucei. *Proc. Natl. Acad. Sci. U.S.A.* 105, 1999–2004. doi: 10.1073/pnas.0711799105

Lanham, S. M., and Godfrey, D. G. (1970). Isolation of salivarian trypanosomes from man and other mammals using DEAE-cellulose. *Exp. Parasitol.* 28, 521–534. doi: 10.1016/0014-4894(70)90120-7

Li, F. J., Gasser, R. B., Zheng, J. Y., Claes, F., Zhu, X. Q., and Lun, Z. R. (2005). Application of multiple DNA fingerprinting techniques to study the genetic relationships among three members of the subgenus *Trypanozoon* (Protozoa: Trypanosomatidae). *Mol. Cell. Probes* 19, 400–407. doi: 10.1016/j.mcp.2005.07.002

Liniger, M., Bodenmuller, K., Pays, E., Gallati, S., and Roditi, I. (2001). Overlapping sense and antisense transcription units in *Tryapnosoma brucei*. *Mol. Microbiol.* 40, 869–878. doi: 10.1046/j.1365-2958.2001.02426.x

Lun, Z. R., Allingham, R., Brun, R., and Lanham, S. M. (1992a). The isoenzyme characteristics of *Trypanosoma evansi* and *Trypanosoma equiperdurm* isolated from domestic stocks in China. *Ann. Trop. Med. Parasitol.* 86, 333–340. doi: 10.1080/00034983.1992.11812675

Lun, Z. R., Brun, R., and Gibson, W. (1992b). Kinetoplast DNA and molecular karyotypes of *Trypanosoma evansi* and *Trypanosoma equiperdum* from China. *Mol. Biochem. Parasitol.* 50, 189–196. doi: 10.1016/0166-6851(92)90215-6

Lun, Z. R., Lai, D. H., Li, F. J., Lukes, J., and Ayala, J. F. (2010). *Tryanosoma brucei*: two steps to spread from Africa. *Trends Parasitol.* 26, 424–427. doi: 10.1016/j.pt.2010.05.007

Lun, Z. R., Lai, D. H., Wen, Y. Z., Zheng, L. L., Shen, J. L., Yang, T. B., et al. (2015). Cancer in the parasitic protozoans *Trypanosoma brucei* and *Toxoplasma gondii*. *Proc. Natl. Acad. Sci. U.S.A.* 112, 8835–8842. doi: 10.1073/pnas.1502599112

Lun, Z. R., Li, A. X., Chen, X. G., Lu, L. X., and Zhu, X. Q. (2004). Molecular profiles of *Trypanosoma brucei*, *T. evansi* and *T. equiperdum* stocks revealed by the random amplified polymorphic DNA method. *Parasitol. Res.* 92, 335–340. doi: 10.1007/s00436-003-1054-8

Matthews, K. R. (2011). Controlling and coordinating development in vector-transmitted parasites. *Science* 331, 1149–1153. doi: 10.1126/science.1198077

Matthews, K. R. (2021). Trypanosome signaling-quorum sensing. *Annu. Rev. Microbiol.* 75, 495–514. doi: 10.1146/annurev-micro-020321-115246

McDonald, L., Cayla, M., Ivens, A., Mony, B. M., MacGregor, P., Silvester, E., et al. (2018). Non-linear hierarchy of the quorum sensing signaling pathway in bloodstream form African trypanosomes. *PLoS Pathogen* 14, e1007145. doi: 10.1371/journal.ppat.1007145

Mony, B. M., and Matthews, K. R. (2015). Assembling the components of the quorum sensing pathway in Africa trypanosomes. *Mol. Microbiol.* 96, 220–232. doi: 10.1111/mmi.12949

Naguleswaran, A., Doiron, N., and Roditi, I. (2018). RNA-Seq analysis validates the use of culture-derived *Trypanosoma brucei* and provides new markers for mammalian and insect life-cycle stages. *BMC Genomics* 19, 227. doi: 10.1186/s12864-018-4600-6

Njiru, Z. K., Constantine, C. C., Masiga, D. K., Reid, S. A., Thompson, R. C. A., and Gibson, W. C. (2006). Characterization of *Trypanosoma evansi* type b. *Infection Genet. Evol.* 6 (4), 292–300. doi: 10.1016/j.meegid.2005.08.002

Oldrieve, G., Verney, M., Jaron, K. S., Hebert, L., and Matthews, K. R. (2021). Monomorphic *Trypanozoon*: towards reconciling phylogeny and pathologies. *Microbial Genomics* 7, 000632. doi: 10.1099/mgen.0.000632

Ou, Y. C., Gioud, C., and Baltz, T. (1991). Kinetoplast DNA analysis of four *Trypanosoma evansi* strains. *Mol. Biochem. Parasitol.* 46, 97–102. doi: 10.1016/0166-6851(91)90203-I

Reuner, B., Vassella, E., Yutzy, B., and Boshart, M. (1997). Cell density triggers slender to stumpy differentiation of *Trypanosoma brucei* bloodstream forms in culture. *Mol. Biochem. Parasitol.* 90, 269–280. doi: 10.1016/S0166-6851(97)00160-6

Richardson, J. P., Beecroft, R. P., Tolson, D. L., Liu, M. K., and Pearson, T. W. (1988). Procyclin: an unusual immunodominant glycoprotein surface antigen from the procyclic stage of African trypanosomes. *Mol. Biochem. Parasitol.* 31, 203–216. doi: 10.1016/0166-6851(88)90150-8

Roditi, I., Furger, A., and Ruepp, S. (1998). Unravelling the procyclin coat of *Trypanosoma brucei*. *Mol. Biochem. Parasitol.* 91, 117–130. doi: 10.1016/S0166-6851(97)00195-3

Rojas, F., Silvester, E., Young, J., Milne, R., Tettey, M., Houston, D. R., et al. (2019). Oligopeptide signaling through TbGPR89 drives trypanosome quorum sensing. *Cell* 176, 306–317. doi: 10.1016/j.cell.2018.10.041

Saldivia, M., Ceballos-Perez, G., Bart, J. M., and Navarro, M. (2016). The AMPK alpha1 pathway positively regulates the developmental transition from proliferation to quiescence in *Trypanosoma brucei*. *Cell Rep.* 17 (3), 660–670. doi: 10.1016/j.celrep.2016.09.041

Schnaufer, A., Domingo, G. J., and Stuart, K. (2002). Natural and induced dyskinetoplastic trypanosomatids: how to live without mitochondrial DNA. *Int. J. Parasitol.* 32, 1071–1084. doi: 10.1016/S0020-7519(02)00020-6

Seed, J. R., and Sechelski, J. B. (1989). Mechanism of long slender (LS) to short stumpy (SS) transformation in the African trypanosomes. *J. Protozool.* 36, 572–577. doi: 10.1111/j.1550-7408.1989.tb01099.x

Silvester, E., Ivens, A., and Matthews, K. R. (2018). A gene expression comparison of *Trypanosoma brucei* and *Trypanosoma congolense* in the bloodstream of the mammalian host reveals species-specific adaptations to density-dependent development. *PLoS Negl. Trop. Dis.* 12, e0006863. doi: 10.1371/journal.pntd.0006863

Suganuma, K., Narantsatsral, S., Battur, B., Yamasaki, S., Otgonsuren, D., Musinguzi, S. P., et al. (2016). Isolation, cultivation and molecular characterization of a new *Trypanosoma equiperdum* strain in Mongolia. *Parasites Vectors* 9, 481. doi: 10.1186/s13071-016-1755-3

Timms, M. W., van Deursen, F. J., Hendriks, E. F., and Matthews, K. R. (2002). Mitochondrial development during life cycle differentiation of African trypanosomes: evidence for a kinetoplast-dependent differentiation control point. *Mol. Biol. Cell* 13, 3747–3759. doi: 10.1091/mbc.e02-05-0266

Vassella, E., Braun, R., and Roditi, I. (1994). Control of polyadenylation and alternative splicing of transcripts from adjacent genes in a procyclin expression site: a dual role for polypyrimidine tracts in trypanosomes? *Nucleic Acids Res.* 22, 1359–1364. doi: 10.1093/nar/22.8.1359

Ventura, R. M., Takata, C. S., Silva, R. A., Nunes, V. L., Takeda, G. F., and Teixeira, M. M. (2000). Molecular and morphological studies of Brazilian *Trypanosoma evansi* stocks: the total absence of kDNA in trypanosomes from both laboratory stocks and naturally infected domestic and wild mammal. *J. Parasitol.* 86, 1289–1298. doi: 10.1645/0022-3395(2000)086[1289:MAMSOB]2.0.CO;2

Verney, M., Grey, F., Lemans, C., Geraud, T., Berthier, D., Thevenon, S., et al. (2020). Molecular detection of 7SL-derived small RNA is a promising alternative for trypanosomosis diagnosis. *Transboundary Emerging Dis.* 67, 3061–3068. doi: 10.1111/tbed.13744

Wen, Y. Z., Lun, Z. R., Zhu, X. Q., Hide, G., and Lai, D. H. (2016). Further evidence from SSCP and ITS DNA sequencing support *Trypanosoma evansi* and *Trypanosoma equiperdum* as subspecies or even strains of *Trypanosoma brucei*. *Infection Genet. Evol.* 41, 56–62. doi: 10.1016/j.meegid.2016.03.022

Wen, Y. Z., Zheng, L. L., Liao, J. Y., Wang, M. H., Wei, Y., Guo, X. M., et al. (2011). Pseudogene-derived small interference RNAs regulate gene expression in African *Trypanosoma brucei*. *Proc. Natl. Acad. Sci. U.S.A.* 108, 8345–8350. doi: 10.1073/pnas.1103894108

Zhang, Z. Q., and Baltz, T. (1994). Identification of *Trypanosoma evansi, trypanosoma equiperdum* and *Tryanpsoma brucei brucei* using repetitive DNA probes. *Veterinary Parasitol.* 53, 197–208. doi: 10.1016/0304-4017(94)90183-X

Zimmermann, H., Subota, I., Batram, C., Kramer, S., Janzen, C. J., Jones, N. G., et al. (2017). A quorum sensing-independent path to stumpy development in *Trypanosoma brucei*. *PLoS Pathog.* 13 (4), e1006324. doi: 10.1371/journal.ppat.1006324